Modular Click Assembly of Degradable Capsules Using Polyrotaxanes

Henk H. Dam and Frank Caruso*

Department of Chemical and Biomolecular Engineering, The University of Melbourne, Victoria 3010, Australia

ABSTRACT

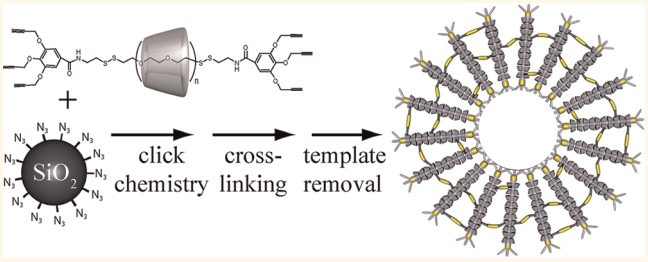

A modular approach for the formation of degradable capsules using polyrotaxanes (PRXs) is described. The PRXs consist of α-cyclodextrin (αCD) and poly(ethylene glycol) (PEG), which are both biologically benign and the main degradation products of the capsules. The PRXs were equipped with three alkyne groups at their ends and could be successfully grafted to azide-functionalized silica particles (2.76 μm diameter) using azide−alkyne click chemistry. The assembled PRXs were then cross-linked using a degradable linker. The cross-linked structure was sufficiently robust to allow the formation of capsules after dissolving the template silica particles. The formation of capsules of *ca.* 2 μm diameter was verified by optical microscopy, TEM, and AFM imaging. The capsules were loaded with the chemotherapy drug doxorubicin (DOX) by conjugating it to the threaded αCDs *via* their free OH groups, while maintaining degradability of the capsules. Alkyne moieties at the surface of the cross-linked PRX architecture were available for further functionalization of the capsules, as is demonstrated by clicking on fluorescent PEG moieties. The DOX-loaded capsules were degraded within 90 min at 37 °C upon exposure to a 5 mM solution of glutathione in water.

KEYWORDS: polyrotaxanes · capsules · drug delivery · click chemistry · cyclodextrin · PEG

Engineering capsules for drug/gene delivery entails the incorporation of a number of essential properties,[1,2] including a nonfouling exterior, targeting groups, and the ability to controllably load and release drugs. Fulfilling these criteria is a challenging task linked to the level of control over the composition, architecture, and function of capsules that can be achieved. A wide range of assembly techniques[3−11] has been used for the preparation of capsules, and often macromolecular building blocks are used as components. The use of α-cyclodextrin (αCD)-poly(ethylene glycol) (PEG) polyrotaxanes (PRXs)[12−14] (herein referred to as PRXs) as macromolecular building blocks for the preparation of capsules is of interest because PRXs exhibit a number of unique and tunable properties[15−17] that can provide control over capsule architecture and function. PRXs are formed *via* a self-assembly process in water, followed by capping of the PEG end groups with bulky groups. This process allows relatively straightforward control over their supramolecular structure and structural properties, such as size, which can be tuned by adjusting the PEG length and their rigidity by varying the threading degree.[18−20] This approach also enables the use of a range of different capping groups, which can be exploited to introduce additional functionalities into the PRXs.[16] The noncovalent nature of the PRX structure is attractive, as it endows them with disassembly properties,[21−25] offering the potential for the formation of degradable capsules. Disassembly can be commenced by uncapping the PRX, upon which the αCDs will dethread. Such dethreading has been achieved using a range of triggers, such as reducing conditions,[21,22] pH changes,[23] enzymes,[24] and UV light.[25] Furthermore, threaded αCDs can be readily postmodified to allow for the introduction of additional functionality such as charged groups[21,26,27] and the conjugation of drugs.[28,29] The latter is advantageous when PRXs are used as building blocks for capsules in drug delivery.

The unique properties of PRXs allow the synthesis of functional degradable polymers that are rigid and highly biocompatible. Inspired by this, we sought to develop responsive nanostructures based on PRX building blocks for therapeutic delivery. Recently, we demonstrated the formation of multilayers using PRXs that can be degraded by initiating the disassembly of the PRXs *via* disulfide bond cleavage.[21] Herein, we report the preparation of PRX capsules with various functionalities within the shell architecture. For fabrication of these

* Address correspondence to fcaruso@unimelb.edu.au.

Received for review November 8, 2011 and accepted May 22, 2012.

Published online May 31, 2012
10.1021/nn301045z

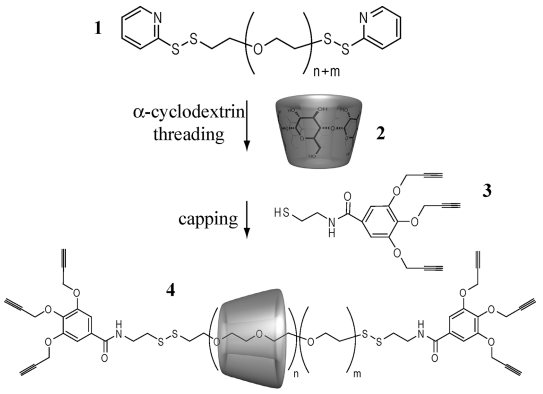

Scheme 1. Formation of PRX 4 by threading of PEG 1 with αCDs, followed by capping the polypseudorotaxane with the trialkyne capping group 3.

capsules we developed a modular assembly approach that relies on the preparation of PRXs in solution prior to their assembly (Scheme 1 and Figure 1). This enables full exploitation of the tunable properties of the PRXs, and, being a major component of the capsules, it provides a means for the preparation of capsules that have specific characteristics and morphologies. The two-step assembly approach reported here also avoids the use of a large number of steps to prepare capsules.

RESULTS AND DISCUSSION

At the base of the modular assembly approach is the Cu(I)-catalyzed Huisgen reaction.[30] This click reaction between alkyne and azide moieties proceeds under mild conditions and yields a highly stable triazole ring, making it attractive for the encapsulation of therapeutics. The high specificity of this reaction also makes it possible to functionalize the capsule surface with a broad range of functional groups to tailor the properties. In related work, we previously reported the click-mediated antibody functionalization of polymer capsules.[31] In the current study, we employ this approach to functionalize the PRX capsules with PEG moieties. The Cu(I)-catalyzed Huisgen reaction has been used previously in combination with CD polyrotaxanes, for example for the functionalization of threaded CDs[32] and for connecting end-capping groups.[33] However, it has not been used for the end-functionalization of PRXs, and, therefore, we designed and prepared PRX **4** with three alkyne moieties at each end-capping group. PRX **4** is the basic component of our modular assembly approach (Scheme 1). The trialkyne capping groups are connected *via* disulfide bonds, making it possible to trigger the disassembly of PRX **4** under reducing conditions. We have used this strategy previously for the reductive degradation of multilayered films comprising PRXs using glutathione (GSH).[21] The main disassembly products of PRX **4** are highly biocompatible αCDs[34] and PEG,[35,36] which is of interest for drug delivery applications. Additionally,

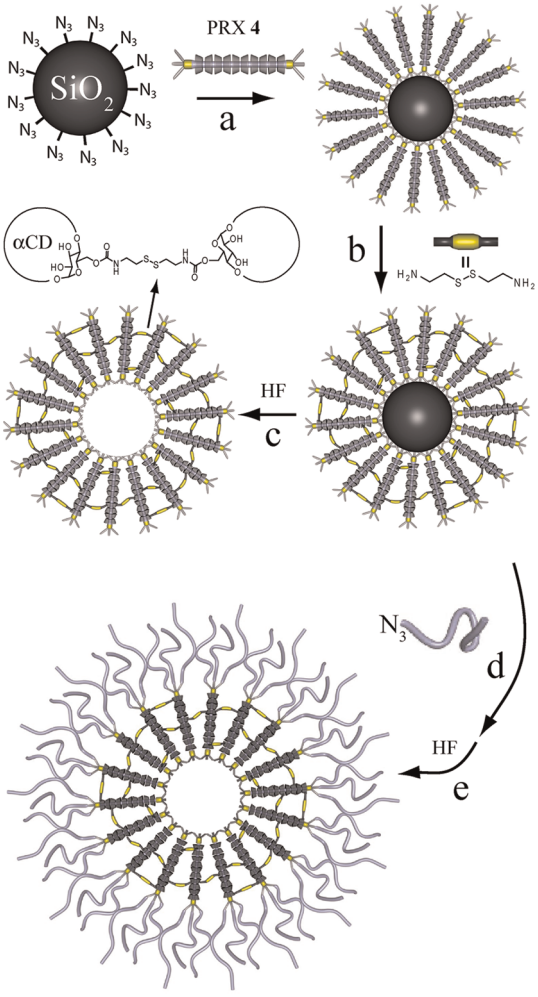

Figure 1. Modular assembly of a degradable PRX capsule using click chemistry. The first step (a) in the assembly is clicking alkyne-modified PRX 4 onto the surface of an azide-functionalized silica template. This is followed by cross-linking of the assembled PRXs with cystamine ($H_2NCH_2CH_2$-$SSCH_2CH_2NH_2$) (b). Capsules are formed by dissolution of the core using buffered HF (c). PEG (M_w 2000)-functionalized capsules can be formed by clicking on PEG-N_3 (d), followed by removal of the core using buffered HF (e).

threaded αCDs offer the possibility of drug conjugation[28] and drug stabilization[37,38] upon release.

PRX **4** was synthesized by starting with commercially available bis(*o*-pyridyldisulfide) poly(ethylene glycol) (OPSS-PEG-OPSS) (**1**) of M_w 3.4 kDa containing activated thiol groups at both ends. The OPSS-PEG-OPSS was threaded with αCDs following the method reported by Harada,[39] in which the PEG is mixed with a concentrated solution of αCD at 24 °C, giving polypseudorotaxanes (PPRXs) as a white precipitate. The PPRXs are soluble in DMF or DMSO; however, solubilization is accompanied by dethreading of the αCDs[40] since αCD-PEG inclusion is largely based on hydrophobic interactions and thus is most efficient in water. PRX formation was, therefore, performed in suspension using a sufficiently fast capping reaction to avoid significant dethreading. Thiol **3** was used as a capping

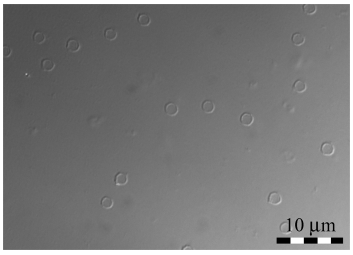

Figure 2. Optical microscopy image of PRX capsules in water (d = 1.9 ± 0.1 μm).

group. On reaction with the PPRX, PRX **4** was formed. The presence of the disulfide groups allows dethreading of these PRXs under reducing conditions.[21] αCD-PEG PRXs are characterized by their insolubility in water, which allows them to be separated from free αCDs and unthreaded PEG chains. In the ^{1}H NMR spectrum of **4**, a characteristic broadening of αCD proton peaks was observed, owing to its reduced mobility in the threaded state.[18] From integration of the areas of the C*H*-1 signal at 4.80 ppm and the CH_2CH_2 protons of the PEG chain at 3.50 ppm, the average number of threaded αCDs was determined to be 31 per PEG chain. The length of two PEG monomeric units corresponds to the cavity size of one αCD.[41] PEG of 3.4 kDa has 76 monomeric units, so the maximum number of αCDs that can be threaded is therefore 38. With 82% of threading, the structure of PRX **4** is rigid and rod-shaped with an approximate length of 28 nm (PEG monomer length = 3.64 Å).[42] The ^{1}H spin−lattice relaxation time (T_1) of the C*H*-1 protons in threaded αCDs is larger (1.50 ± 0.043 s) than that of the C*H*-1 protons of free αCD (1.09 ± 0.009 s) in solution, which corresponds to the decreased mobility of the threaded αCDs in PRX **4**. The characteristic broad signals due to the threaded αCDs disappeared when 5 mM GSH was added and the OH-2 and OH-3 signals from αCD shifted to higher field, 5.66 to 5.55 ppm and 5.50 to 5.46 ppm, respectively, confirming disassembly of the PRX by reductive cleavage of the disulfide bonds.

The modular assembly is commenced by clicking PRX **4** onto the surface of azide-modified silica particles[43] that are used as templates (Figure 1, step a). To prevent cross-linking of particles, an excess of PRX was used in the reaction (see Methods section). After the assembly, no aggregates were observed, indicating a negligible degree of cross-linking. The assembled PRXs are cross-linked using cystamine, which is biocleavable, as it contains a central disulfide moiety (Scheme S2). We note that it is difficult to avoid intramolecular cross-linking of αCDs within the same PRX. However, cross-linking of the assembled PRXs results in the formation of a stable architecture, sufficiently robust to allow capsule formation following dissolution of the particle core with buffered hydrofluoric acid (HF) (Figure 2). This indicates that there is significant intermolecular cross-linking between the PRXs. The reactivity of buffered HF toward PRX **4** was examined by exposing the PRX to similar conditions to those used for template particle removal. Analysis of the HF-exposed PRX **4** by ^{1}H NMR showed that no significant reaction took place. Previous studies in our group have also shown that capsules consisting of organic polymers, including PEG, formed by template removal using buffered HF retain their functionality (*e.g.*, pH swelling and responsiveness to disulfide cleavage).[44] The diameter of the PRX capsules formed is 1.9 ± 0.1 μm, determined by optical microscopy, which is ∼30% less than that of the template SiO_2 particles (2.8 μm). The shrinkage of the capsules on dissolution of the template could be explained by a less than optimum percentage of intermolecular cross-linking. This would reduce the rigidity of the capsule wall since there would be more mobility and space in the capsule wall. It is notable, however, that some degree of mobility will be present due to the rotational freedom of threaded αCDs and their lateral mobility. The latter is dependent on the threading degree and is relatively small for PRX **4**, which has a threading degree of 82%.

The size of the capsules was confirmed by TEM and AFM imaging (Figure 3). In these images folds are visible, which is characteristic of air-dried polymer capsules.[45] From the height profiles of the AFM images a minimum thickness of approximately 9 nm was found. This number should not be considered to be representative of the average thickness of the capsule wall since air drying the capsules could introduce defects. It is possible for the PRXs to assemble parallel on the surface *via* the reaction of both alkyne end-capping groups of one PRX to the surface. The excess of PRX used in the assembly process, in combination with the efficiency of the click reaction, would, however, minimize this. From the AFM results it can be concluded that this side reaction is not significant, as it would lead to a smaller wall thickness than that observed (thickness of PRX ∼2 nm). A less than optimum percentage of intermolecular cross-linking in combination with less than 100% assembly efficiency of the PRXs onto the template surface is likely to contribute to a tilted orientation of the PRXs with respect to the surface, leading to a thinner capsule wall (Figure 3c) (the maximum thickness of the capsule wall would be ∼30 nm, which corresponds to the length of PRX **4**).

Due to the rigidity of PRX **4**, back bending of the assembled PRXs is not possible, which means that the remaining alkyne groups are mostly located at the outer area of the capsule wall. This also indicates that even when there is a tilted orientation of PRXs on the surface, it is still possible to obtain capsules with distinct surface functionalities. The alkyne moieties are accessible for further functionalization and allow the preparation of capsules with a range of properties

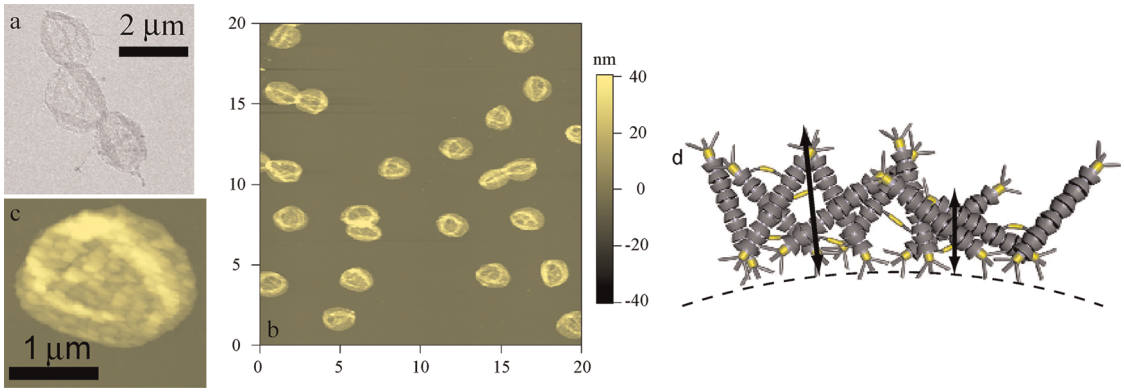

Figure 3. (a) TEM image and (b, c) AFM images of air-dried capsules. For (b), the *x* and *y* scales are in micrometers. (d) Illustration of a capsule wall in which the PRXs are organized in a tilted fashion. The lines indicate the differences in wall thicknesses.

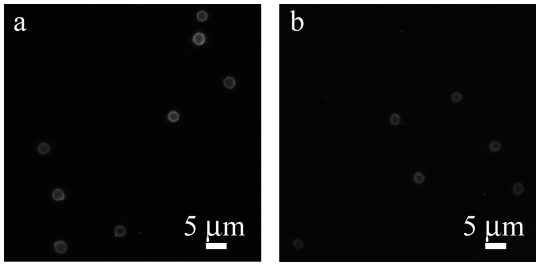

Figure 4. Fluorescence microscopy images of (a) capsules functionalized with PEG-AF633 *via* click chemistry ($d = 2.6 \pm 0.2$ μm) and (b) capsules with DOX conjugated to the threaded αCDs ($d = 2.0 \pm 0.2$ μm).

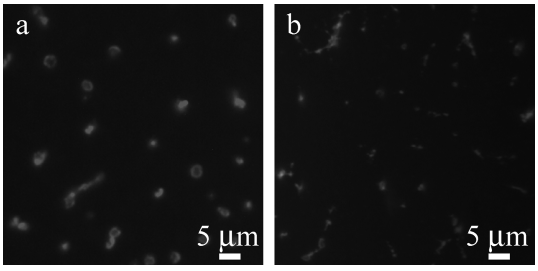

Figure 5. Fluorescence microscopy images of the degradation of DOX-loaded capsules taken after (a) 30 min and (b) 90 min. No capsules were observed after 3 h.

using the mild and specific click reaction. The mild conditions used for the click reaction are essential, as they enable the nondestructive conjugation of biomolecules to a capsule.[31] Here, we prepared capsules functionalized with PEG (M_w 2000), as it can impart biological nonfouling behavior.[35] Heterobifunctional azide-PEG2000-NHS was functionalized with a fluorescent dye containing a hydrazide moiety (AF633-hydrazide) to give PEG2k-633 (Scheme S3). The dye-modified PEG was clicked onto the assembled PRXs followed by a number of washing steps (Figure 1, steps d and e). Dissolution of the template core gave fluorescent capsules, indicating the presence of PEG moieties (Figure 4a). The diameter of these capsules was 2.6 ± 0.2 μm, which was 37% larger than that of the nonfunctionalized capsules. These capsules shrink less as result of the presence of the bulky PEG moieties.

Threaded αCDs in the cross-linked PRX architecture contain free hydroxyl groups that can be used for loading the capsule wall with drugs. We conjugated doxorubicin (DOX) to the OH groups of threaded αCDs after step b (Figure 1). The conjugation was performed by activating the hydroxyl groups with *N*,*N*-disuccinimidyl carbonate (diNHS), followed by the addition of DOX, upon which a stable carbamate bond is formed. After dissolution of the cores, fluorescent capsules were obtained due to the inherent fluorescence of DOX (Figure 4b). This strategy not only creates an opportunity for loading the capsules with small therapeutics but also opens a possible route for the chemical modification of the capsule wall interior to tune its properties, for example, with charged groups, lipophilic groups, or ligands. Furthermore, the successful functionalization of the threaded αCDs with DOX also shows that there are a significant number of free OH groups present on the αCDs.

The degradation of the DOX-loaded capsules was performed in 5 mM GSH. GSH, which is present within cells at concentrations up to 5 mM,[46] is capable of cleaving disulfide bonds and is used to mimic intracellular conditions. Cleavage of the disulfide bonds present in the capsules releases DOX-αCD conjugates *via* dethreading. Fluorescence microscopy showed that after exposure to 5 mM GSH for 3 h at 37 °C no capsules were present. During the degradation process the capsules first deform (Figure 5a) and then collapse (Figure 5b), upon which they degrade. In order to obtain an indication of the amount of DOX released upon degradation of the capsules, the fluorescence of the supernatant after capsule degradation was measured. The amount of DOX released per capsule was calculated to be approximately $\sim 2 \times 10^{-5}$ ng; for a capsule with a diameter of 2 μm the concentration of DOX per capsule was 1×10^{-3} M. Our previous studies have shown that the IC_{50} of DOX to colorectal cancer cell lines was $\sim 10^{-6}$.[47] Furthermore, it has been shown that efficient delivery of DOX to cells *via* capsules can

increase the efficacy of the drug by more than 5 orders of magnitude.[48] Therefore it can be concluded that an effective dose of DOX can be released by the PRX capsules.

CONCLUSION

In conclusion, we have reported a modular, two-step assembly approach for the preparation of capsules using click chemistry and PRXs as components. We have demonstrated that the modular approach allows the preparation of surface-functionalized capsules and loading with DOX *via* conjugation to the threaded αCDs. These capsules maintain their degradability, during which process the αCD-DOX conjugates are released. The use of tunable PRXs in combination with click chemistry for postfunctionalization will enable the preparation of capsules that are finely tuned with respect to their structure, composition, and functionality, thus making these PRX capsules of interest for a broad range of applications.

MATERIALS AND METHODS

General Methods. The pH of all solutions was measured with a Mettler-Toledo MP220 pH meter. High-purity water with a resistivity of >18 $\Omega M \cdot cm^{-1}$ was obtained from an inline Millipore RiOs/Origin water purification system. Silicon wafers were obtained from MMRC Pty (Melbourne, Australia). αCD, dimethylformamide (DMF), dimethylsulfoxide (DMSO), methylene chloride (CH_2Cl_2), methanol (MeOH), glutathione (GSH), cystamine dihydrochloride, dithiothreitol (DTT), doxorubicin hydrochloride, and triethylamine were obtained from Sigma-Aldrich. *N,N′*-Disuccinimidyl carbonate (diNHS) was obtained from Fluka, heterobifunctionalized azido-poly(ethylene glycol)-*N*-hydroxysuccinimide (N_3-PEG-NHS), M_w 2 kDa, from JenKem, Alexa Fluor 633 hydrazide (AF633) dye from Life Technologies, Inc., and homobifunctionalized *o*-pyridyldisulfide-poly(ethylene glycol) (OPSS-PEG-OPSS), M_w 3.4 kDa, from Creative PEGWorks. Methyl 3,4,5-tris(prop-2-yn-1-yloxy)benzoate (**5**) was synthesized according to a procedure previously reported.[49] All chemicals were used as received. (See Scheme S1 for synthetic conditions.) SiO_2 microparticles (2.76 ± 0.15 μm diameter) were obtained from Microparticles GmbH as a 50 mg mL^{-1} dispersion in water. Analytical TLC was performed using Merck prepared plates (silica gel 60 F-254 on aluminum). Column chromatography was carried out on Merck silica gel 60 (230−400 mesh). Melting points were measured with a Selbys melting point apparatus. Thermal properties of the PRXs were measured on a Perkin-Elmer Diamond differential scanning calorimetry instrument. Spectra were recorded from −50 to 350 °C at 5 °C per min. Nuclear magnetic resonance (NMR) spectra were recorded using a 400 MHz Varian INOVA system at 25 °C. The spin−lattice relaxation time (T_1) was determined at 24 °C *via* a conventional inversion recovery pulse sequence, 90°−τ−180°, under deuterium lock mode. Spectra were referenced to residual proton resonances of the deuterated solvent. Chemical shifts are reported as parts per million (ppm) downfield from the signal originating from TMS. High-resolution quadrupole time-of-flight mass spectrometry measurements were performed on an Agilent Q-Tof 6520 with an electrospray ionization (ESI) source. FTIR spectroscopy was carried out on a Bruker Vector 22 FTIR spectrophotometer. The spectra were measured in the range 4000−400 cm^{-1}. The spectra were collected by cumulating 16 scans at a resolution of 4 cm^{-1}. Differential interference contrast (DIC) and fluorescence images were taken on an inverted Olympus IX71 microscope equipped with a DIC slider (U-DICT, Olympus) with a 60× objective lens (Olympus UPFL20/0.5 NA, W.D. 1.6). A CCD camera (bw) was mounted on the left-hand port of the microscope. A tungsten lamp was used for DIC images. Fluorescence images were illuminated with an Hg arc lamp, using a UF1032 filter cube. The fluorescence intensity of doxorubicin released (excitation 480 nm, emission 580 nm) was measured using a Horiba Fluorolog spectrophotometer using a 200 μL quartz cuvette and based on an absorbance calibration curve.

Synthesis. *3,4,5-Tris(prop-2-yn-1-yloxy)benzoic Acid (6).* A solution of methyl 3,4,5-tris(prop-2-yn-1-yloxy)benzoate (**5**) (3.00 g, 10.1 mmol) and sodium hydroxide (2.01 g, 50.3 mmol) in 50 mL of MeOH and 10 mL of H_2O was stirred at 40 °C for 2 h. After the reaction was completed, HCl(aq) (12.1 mL, 5 M) was added, and the mixture was slowly cooled to 24 °C, upon which white crystals formed. The crystals were washed with 3 × 50 mL of H_2O and freeze-dried, giving 2.8 g of pure product (98% yield): mp 147 °C. ^{1}H NMR (DMSO-d_6): δ 7.38 (s, 2H, Ph); 4.89 (d, J = 2.0 Hz, 4H, CH_2); 4.71 (d, J = 2.0 Hz, 2H, CH_2); 3.61 (t, J = 2.0 Hz, 2H, CH); 3.47 (t, J = 2.0 Hz, 1H, CH). ^{13}C NMR (DMSO-d_6): δ 166.8 (CO); 151.0 (2 × ArC); 139.8 (ArC); 126.4 (ArC); 109.0 (2 × ArC); 79.2 (C); 79.0 (2 × C); 78.8 (2 × CH); 78.4 (CH); 59.6 (CH_2); 56.6 (2 × CH_2). High-resolution MS (ESI$^+$): calcd for $[M + H]^+$, 285.0765; found, 285.0405.

N-Hydroxysuccinimidyle-3,4,5-tris(prop-2-yn-1-yloxy)-benzoate (7). A solution of **6** (1.70 g, 0.596 mmol), diNHS (1.53 g, 0.596 mmol), and triethylamine (0.830 mL, 0.596 mmol) was stirred at 24 °C in 20 mL of DMF for 18 h. The volatiles were removed under reduced pressure at 40 °C. The crude product was purified using column chromatography and collected as the first fraction (eluent MeOH/CH_2Cl_2, 1:40, R_f = 0.8 on TLC). The product was crystallized from the eluent as white needles, which were washed with cold MeOH (5 °C), affording 1.45 g, 64%; mp 111 °C. ^{1}H NMR ($CDCl_3$): δ 7.54 (s, 2H, Ph); 4.86 (d, J = 2.4 Hz, 4H, CH_2); 4.80 (d, J = 2.4 Hz, 2H, CH_2); 2.90 (s, 4H, CH_2CH_2); 2.55 (t, J = 2.4 Hz, 2H, CH); 2.47 (t, J = 2.4 Hz, 1H, CH). ^{13}C NMR ($CDCl_3$): δ 169.3 (NHCO); 161.3 (CO); 151.7 (2 × ArC); 142.9 (ArC); 120.4 (ArC); 111.0 (2 × ArC); 78.4 (C); 77.7 (2 × C); 76.8 (2 × CH); 76.1 (CH); 60.5 (CH_2); 57.4 (2 × CH_2); 25.8 (CH_2CH_2). High-resolution MS (ESI$^+$): calcd for $[M + H_2O]^+$, 399.0955; found, 399.0930.

2,2′-Dithiobisethanamino-3,4,5-tris(prop-2-yn-1-yloxy)-benzamide (8). To a solution of **7** (0.720 g, 0.188 mmol) in 10 mL of CH_2Cl_2 was added a solution of cystamine·2HCl (0.211 g, 0.939 mmol) and triethylamine (0.50 mL) in 10 mL of MeOH. The resulting mixture was stirred at 24 °C for 18 h. The volatiles were removed under reduced pressure at 40 °C, and the crude product was dissolved in 30 mL of CH_2Cl_2 and washed with 20 mL of 0.001 M HCl and 2 × 30 mL of H_2O. The organic layer was dried with $MgSO_4$. The volatiles were removed under reduced pressure at 24 °C, affording pure **8** as a white compound (0.550 mg, 68%); mp 114 °C. ^{1}H NMR ($CDCl_3$): δ 7.27 (s, 4H, Ph); 7.06 (t, J = 4.4 Hz, 2H, NH); 4.79 (d, J = 2.0 Hz, 4H, CH_2); 4.75 (d, J = 1.6 Hz, 4H, CH_2); 3.80 (q, J = 5.2 Hz, 4H, CH_2N); 3.01 (t, J = 5.2 Hz, 4H, SCH_2); 2.51 (t, J = 2.0 Hz, 4H, CH); 2.46 (t, J = 2.0 Hz, 2H, CH). ^{13}C NMR ($CDCl_3$): δ 167.2 (NHCO); 151.6 (2 × ArC); 130.1 (ArC); 108.0 (3 × ArC); 78.9 (C); 78.2 (2 × C); 76.4 (2 × CH); 75.8 (CH); 60.5 (CH_2); 57.3 (2 × CH_2); 39.7 (CH_2N); 38.1 ($SSCH_2$). High-resolution MS (ESI$^+$): calcd for $[M + H]^+$, 685.1680; found, 685.1524.

2-Mercaptoethyl-3,4,5-tris(prop-2-yn-1-yloxy)benzamide (3). A solution of **8** (0.150 g, 0.219 mmol), DTT (0.135 g, 0.876 mmol), and triethylamine (0.122 mL, 0.438 mmol) was stirred at 24 °C in 20 mL of CH_2Cl_2 for 2.5 h. The organic layer was washed with H_2O (4 × 20 mL) and dried with $MgSO_4$. The volatiles were removed under reduced pressure at 24 °C, affording pure **3** as a white compound, 0.149 g, 99%; mp 83 °C. ^{1}H NMR ($CDCl_3$): δ 7.21 (s, 2H, Ph), 6.51 (b, 1H, NH), 4.81 (d, J = 2.0 Hz, 4H, CH_2); 4.80 (d, J = 2.0 Hz, 2H, CH_2); 3.64 (q, J = 4.8 Hz, 2H, CH_2N); 2.80 (m, 2H, SCH_2); 2.54 (t, J = 2.0 Hz, 2H, CH); 2.46 (t, J = 2.0 Hz, 1H, CH); 1.41

(t, J = 2.8 Hz, 1H, SH). ^{13}C NMR ($CDCl_3$): δ 166.8 (NHCO); 151.6 (2 × ArC); 130.3 (ArC); 109.8 (ArC); 107.8 (2 × ArC); 78.8 (C); 78.1 (2 × C); 76.5 (2 × CH); 75.8 (CH); 60.4 (CH_2); 57.3 (2 × CH_2); 43.0 (CH_2N); 24.7 ($HSCH_2$). High-resolution MS (ESI$^+$): calcd for $[M + H]^+$, 344.0958; found, 344.0643.

Polyrotaxane 4. OPSS-PEG-OPSS 3.4k (0.089 g, 0.026 mmol) was dissolved in 0.5 mL of H_2O. The PEG solution was added to a concentrated solution of αCD (1.94 g, 1.99 mmol) in 18 mL of H_2O. Within several minutes a white precipitate was formed, indicating the formation of PPRX assemblies. The suspension was ultrasonicated for 1.5 h followed by shaking overnight at 24 °C. The precipitate was collected by centrifugation at 5000*g* for 5 min, and the supernatant was decanted. Freeze-drying gave 0.960 g of PPRX as a white powder, which contained a fraction of nonthreaded αCD. Compound **3** (0.010 g, 0.029 mmol) was mixed with 0.150 g of PPRX in a 2.0 mL vial. DMF (0.15 mL) was added, upon which the mixture was vortexed until a thick yellow suspension was formed (within minutes). The suspension was ultrasonicated for 1.5 h, upon which 1.5 mL of acetone was added, and the precipitate was washed with 5 × 1.5 mL of acetone (until the washing was colorless) and with 4 × 1.5 mL of H_2O. The crude product was dissolved in 2.0 mL of DMSO and precipitated with 2.0 mL of H_2O. This cycle was repeated five times to ensure that all nonthreaded αCDs and PEG were removed. The precipitate was freeze-dried to give 0.082 g of PRX **4** as a white powder: T_g 145 °C; T_c 157 °C; T_m 283 °C. ^{1}H NMR (500 MHz, DMSO-d_6): (s, 4H, Ph); 5.66 (s, br, 6H, OH-2 of αCD); 5.50 (s, br, 6H, OH-3); 4.80 (s, br, 6H, H-1 of αCD); 4.43 (s, br, 6H, OH-6 of αCD); 3.74−3.27 (m, br, 78H, H-6a,b, H-3, H-5, H-4, H-3 of αCD, OCH_3); 3.51 (s, 304H, $-OCH_2CH_2O-$ of PEG). The number of threaded αCDs per PEG chain was determined to be 31 by integration of the CH-1 signal at 4.80 ppm and the CH_2CH_2 (PEG) protons at 3.51 ppm. ^{13}C NMR (DMSO-d_6): δ 102.0 (C-1 αCD); 82.1 (C-4 αCD); 73.4 (C-3 αCD); 72.1 (C-5 αCD); 71.6 (C-2 αCD); 69.8 (CH_2CH_2-O); 69.4 (br, complexed CH_2CH_2-O);[50] 59.6 (C-6 αCD). IR: ν (cm^{-1}) 3431 (s, br) (O−H αCD); 2924 (s) (C−H αCD); 2255 (s, br) (C≡C). The number of threaded αCDs was verified by disassembling PRX **4** with GSH in D_2O at 24 °C for 18 h and by comparing the integrated values of the PEG signal and the CH-1 signal arising from αCD.

Azide-Functionalized Silica Particles. The silica particles were functionalized with azide groups according to a method described previously.[43] Briefly, silica particles (d = 2.76 μm) were activated by heating at 120 °C under vacuum (10^{-2} mbar) for 24 h. The activated silica particles (0.385 g) were suspended in a solution of 3-azidopropyltrimethoxysilane (0.770 mL) in dry toluene (15 mL). The reaction mixture was refluxed for 48 h. The progress of the reaction was monitored by dispersing a sample of the particles in a mixture of DMSO/Et_3N. Partly functionalized silica particles reside in the DMSO layer, whereas fully functionalized silica particles reside in the top Et_3N layer. The fully azide-functionalized silica particles could not be dispersed in H_2O. However, it is critical that the particles contain a sufficient number of azide groups on the surface, since the formation of capsules starting with silica particles having a low degree of azide functionalization was not possible.

Capsule Preparation. A dispersion of azide-functionalized silica particles (2.5×10^{-3} g, ~1.0×10^8 particles), PRX **4** (2×10^{-3} g), $CuSO_4$ (2.5×10^{-4} g), sodium ascorbate (4.8×10^{-4} g), and chelator **9**[31] (6.3×10^{-4} g) in 380 μL of DMSO was shaken at 24 °C for 18 h at 1500*g*. In this reaction, an excess of PRX relative to the available particle surface area is used. The surface area of a particle (d = 2.76 μm) equals 2.39×10^9 Å^2. The minimum surface area of PRX when assembled perpendicular onto a surface equals the ring-surface area of one αCD and is 491 Å^2. From this it can be calculated that the maximum number of PRXs that can be assembled onto the surface of one particle is ~4.87×10^6. For 2.5 mg of particles, therefore, a minimum of 4.97×10^{14} PRX molecules are required. A 2×10^{-3} g amount of PRX corresponds to 3.54×10^{16} PRX molecules (M_w ~34 000), giving an excess of more than 70 PRXs per one available "grafting to" surface area on each particle. The color of the dispersion was green. The particles were collected by centrifugation (60 s, 2000*g*) and washed in total four times with 500 μL of DMSO. The particles were suspended in 200 μL of DMSO, diNHS (2.1×10^{-3} g) was added, and the resulting mixture was shaken at 24 °C for 1.5 h at 1500*g* (Scheme S2). The particles were collected by centrifugation (60 s, 2000*g*), and the solvent was removed. A solution of cystamine·HCl (3.4×10^{-3} g) in 200 μL of DMSO was added, and the dispersion was shaken at 24 °C for 18 h at 1500*g*. The particles were collected by centrifugation (60 s, 2000*g*), washed in total four times with 500 μL of DMSO, and redispersed in 200 μL of H_2O. Capsules were formed by dissolution of the silica template using a 1:2 mixture of 5 M HF and 13.3 M NH_4F (Figure 2 and Figure S1a) according to a published method, where it was shown that the SiO_2 is effectively dissolved and removed by this method.[51] A sample of 3.3 mg of PRX **4** was dissolved in 100 μL of DMSO, and to this was added 100 μL of a 1:2 mixture of 5 M HF and 13.3 M NH_4F. A gel was formed immediately, and after 5 min PRX **4** was isolated by centrifugation and washed several times with water. The ^{1}H NMR spectrum of this PRX **4** was similar to that of the starting spectrum, indicating that the buffered HF does not significantly react with the PRX.

Preparation of PEG-Functionalized Capsules. A solution of *N*-hydroxysuccinimide-PEG-azide (M_w 2000 Da, 1.74×10^{-4} g) and AF633 hydrazide (2.0×10^{-6} g, ~1/5 equivalent) was shaken at 1500*g* for 2 h at 24 °C in 20 μL of dry DMSO. This PEG-AF633 solution was used without purification. A dispersion of cross-linked PRX particles (2.5×10^{-3} g, obtained after step b (Figure 1)), PEG-AF633 solution (1 μL), $CuSO_4$ (2.5×10^{-4} g), sodium ascorbate (5.0×10^{-4} g), and chelator **9**[4] (6.3×10^{-4} g) in 150 μL of DMSO was shaken at 24 °C for 18 h at 1500*g*. The particles were collected by centrifugation (60 s, 2000*g*) and washed in total four times with 200 μL of DMSO. The particles were suspended in 200 μL of H_2O before analysis with fluorescence microscopy. To verify that the attachment of PEG-AF633 was not the result of nonspecific interaction, a sample was run under the same conditions but without the addition of $CuSO_4$. The capsules of this experiment were not fluorescent.

Loading of Capsules with DOX and Degradation. *N,N*-Disuccinimidyl carbonate (6.0×10^{-3} g) and triethylamine (50 μL) were added to a suspension of cross-linked PRX particles (2.5 mg, obtained after step **b** (Figure 1)) in 200 μL of DMSO, and the resulting mixture was shaken at 24 °C for 1.5 h at 1500*g*. The particles were collected by centrifugation (60 s, 2000*g*), the solvent was removed, and the particles were washed with 200 μL of DMSO. A 10 mM 200 μL DMSO solution of doxorubicin·HCl was added, and the dispersion was shaken at 24 °C for 18 h at 1500*g*. The particles were collected by centrifugation (60 s, 2000*g*), washed in total six times with 200 μL of DMSO, and redispersed in 200 μL of H_2O. Capsules were formed by dissolution of the silica template using a 1:2 mixture of 5 M HF and 13.3 M NH_4F (Figure 2). To verify that the attachment of doxorubicin was not the result of nonspecific interactions, a sample was run under the same conditions, but without the addition of diNHS. The capsules of this experiment were not fluorescent. A dispersion of doxorubicin-loaded capsules in 5 mM GSH in H_2O was shaken at 37 °C at 1500*g*. Samples of 1 μL were taken out at intermittent time intervals and analyzed using fluorescence microscopy (Figure 5). Under the same conditions without GSH the capsules were stable for >72 h.

Atomic Force Microscopy (AFM). AFM images were obtained with an MFP-3D Asylum Research instrument. Typical scans were conducted in ac mode with ultrasharp SiN gold-coated cantilevers (NT-MDT). Samples were prepared by dropping 1 μL of a concentrated particle solution on a freshly cleaned silicon wafer slide followed by dissolving the cores with a 1:2 mixture of 5 M HF and 13.3 M NH_4F and several washing steps. The samples were left to dry before the measurements commenced.

Transmission Electron Microscopy (TEM). TEM images were obtained with a FEI Technai F30 transmission electron microscope operated at 200 kV. Samples were prepared by dropping 1 μL of a concentrated particle solution on carbon-coated 300 mesh copper grids (ProSciTech, Australia) followed by treatment with 5 M HF in 13.3 M NH_4F buffer for 5 min, after which they were thoroughly cleaned with water.

Conflict of Interest: The authors declare no competing financial interest.

Acknowledgment. The ARC is acknowledged for funding under the Federation Fellowship (FF0776078) (F.C.) and Discovery Project (DP0877360) schemes (F.C.).

Supporting Information Available: Synthetic conditions, synthetic steps for cross-linking the capsules, synthetic steps for preparing the capsules, and NMR spectra. This material is available free of charge *via* the Internet at http://pubs.acs.org.

REFERENCES AND NOTES

1. Sukhorukov, G. B.; Möhwald, H. Multifunctional Cargo Systems for Biotechnology. *Trends Biotechnol.* **2007**, *25*, 93–98.
2. Matsusaki, M.; Akashi, M. Functional Multilayered Capsules for Targeting and Local Drug Delivery. *Expert Opin. Drug Delivery* **2009**, *6*, 1207–1217.
3. Lensen, D.; Vriezema, D. M.; van Hest, J. Polymeric Microcapsules for Synthetic Applications. *Macromol. Biosci.* **2008**, *8*, 991–1005.
4. Yoon, H.-J.; Jang, W.-D. Polymeric Supramolecular Systems for Drug Delivery. *J. Mater. Chem.* **2010**, *20*, 211–222.
5. Moughton, A. O.; O'Reilly, R. K. Using Metallo-Supramolecular Block Copolymers for the Synthesis of Higher Order Nanostructured Assemblies. *Macromol. Rapid Commun.* **2010**, *31*, 37–52.
6. Wang, Y.; Hosta-Rigau, L.; Lomas, H.; Caruso, F. Nanostructured Polymer Assemblies Formed at Interfaces: Applications from Immobilization and Encapsulation to Stimuli-Responsive Release. *Phys. Chem. Chem. Phys.* **2011**, *13*, 4782–5188.
7. Johnston, A. P. R.; Cortez, C.; Angelatos, A. S.; Caruso, F. Layer-by-Layer Engineered Capsules and Their Applications. *Curr. Opin. Colloid Interface Sci.* **2006**, *11*, 203–209.
8. De Cock, L. J.; De Koker, S.; De Geest, B. G.; Grooten, J.; Vervaet, C.; Remon, J. P.; Sukhorukov, G. B.; Antipina, M. N. Polymeric Multilayer Capsules in Drug Delivery. *Angew. Chem., Int. Ed.* **2010**, *49*, 6954–6973.
9. Dongen, S. F. M.; de Hoog, H. M.; Peters, R. J. R. W.; Nallani, M.; Nolte, R. J. M.; van Hest, J. C. M. Biohybrid Polymeric Capsules. *Chem. Rev.* **2009**, *109*, 6212–6274.
10. del Mercato, L. L.; Rivera-Gil, P.; Abbasi, A. Z.; Ochs, M.; Ganas, C.; Zins, I.; Sönnichsen, C.; Parak, W. J. LbL Multilayer Capsules: Recent Progress and Future Outlook for Their Use in Life Sciences. *Nanoscale* **2010**, *2*, 458–467.
11. Wu, Y.; Li, J. Synthesis of Supramolecular Nanocapsules Based on Threading of Multiple Cyclodextrins over Polymers on Gold Nanoparticles. *Angew. Chem., Int. Ed.* **2009**, *48*, 3842–3845.
12. Harada, A.; Hashidzume, A.; Yamaguchi, H.; Takashima, Y. Polymeric Rotaxanes. *Chem. Rev.* **2009**, *109*, 5974–6023.
13. Harada, A.; Takashima, Y.; Yamaguchi, H. Cyclodextrin-Based Supramolecular Polymers. *Chem. Soc. Rev.* **2009**, *38*, 875–882.
14. Wenz, G.; Han, B. H.; Mueller, A. Cyclodextrin Rotaxanes and Polyrotaxanes. *Chem. Rev.* **2006**, *106*, 782–817.
15. Li, J.; Loh, X. J. Cyclodextrin-Based Supramolecular Architectures: Synthesis, Structures, and Applications for Drug and Gene Delivery. *Adv. Drug Delivery Rev.* **2008**, *60*, 1000–1017.
16. Loethen, S.; Kim, J.; Thompson, D. H. Biomedical Applications of Cyclodextrin Based Polyrotaxanes. *Polym. Rev.* **2007**, *47*, 383–418.
17. Araki, J.; Ito, K. Recent Advances in the Preparation of Cyclodextrin-Based Polyrotaxanes and Their Application to Soft Materials. *Soft Matter* **2007**, *3*, 1456–1473.
18. Zhao, T.; Beckham, H. W. Direct Synthesis of Cyclodextrin-Rotaxanated Poly(ethylene glycol)s and Their Self-Diffusion Behavior in Dilute Solution. *Macromolecules* **2003**, *36*, 9859–9865.
19. Jarroux, N.; Guégan, P.; Cheradame, H.; Auvray, L. High Conversion Synthesis of Pyrene End Functionalized Polyrotaxane Based on Poly(ethylene oxide) and α-Cyclodextrins. *J. Phys. Chem. B* **2005**, *109*, 23816–23822.
20. Fleury, G.; Brochon, C.; Schlatter, G.; Bonnet, G.; Lapp, A.; Hadziioannou, G. Synthesis and Characterization of High Molecular Weight Polyrotaxanes: Towards the Control over a Wide Range of Threaded α-Cyclodextrins. *Soft Matter* **2005**, *1*, 378–385.
21. Dam, H. H.; Caruso, F. Construction and Degradation of Polyrotaxane Multilayers. *Adv. Mater.* **2011**, *23*, 3026–3029.
22. Ooya, T.; Choi, H. S.; Yamashita, A.; Yui, N.; Sugaya, Y.; Kano, A.; Maruyama, A.; Akita, H.; Ito, R.; Kogure, K. Biocleavable Polyrotaxane-Plasmid DNA Polyplex for Enhanced Gene Delivery. *J. Am. Chem. Soc.* **2006**, *128*, 3852–3853.
23. Loethen, S.; Ooya, T.; Choi, H. S.; Yui, N.; Thompson, D. H. Synthesis Characterization, and pH-Triggered Dethreading of α-Cyclodextrin-Poly(ethylene glycol) Polyrotaxanes Bearing Cleavable Endcaps. *Biomacromolecules* **2006**, *7*, 2501–2506.
24. Yui, N.; Ooya, T.; Kumeno, T. Effect of Biodegradable Polyrotaxanes on Platelet Activation. *Bioconjugate Chem.* **1998**, *9*, 118–125.
25. Taura, D.; Li, S.; Hashidzume, A.; Harada, A. Formation of Side-Chain Hetero-Polypseudorotaxane Composed of α- and β-Cyclodextrins with a Water-Soluble Polymer Bearing Two Recognition Sites. *Macromolecules* **2010**, *43*, 1706–1713.
26. Araki, J.; Ito, K. Polyrotaxane Derivatives. I. Preparation of Modified Polyrotaxanes with Nonionic Functional Groups and Their Solubility in Organic Solvents. *J. Polym. Sci. A: Polym. Chem.* **2006**, *44*, 6312–6323.
27. Yang, C.; Wang, X.; Li, H.; Goh, S. H.; Li, J. Synthesis and Characterization of Polyrotaxanes Consisting of Cationic α-Cyclodextrins Threaded on Poly[(ethylene oxide)-*ran*-(propylene oxide)] as Gene Carriers. *Biomacromolecules* **2007**, *8*, 3365–3374.
28. Moon, C.; Kwon, Y. M.; Lee, W. K.; Park, Y. J.; Yang, V. C. *In Vitro* Assessment of a Novel Polyrotaxane-Based Drug Delivery System Integrated with a Cell-Penetrating Peptide. *J. Controlled Release* **2007**, *124*, 43–50.
29. Joung, Y.; Sengoku, Y.; Ooya, T.; Park, K. D.; Yui, N. Anticoagulant Supramolecular-Structured Polymers: Synthesis and Anticoagulant Activity of Taurine-Conjugated Carboxyethylester-Polyrotaxanes. *Sci. Technol. Adv. Mater.* **2005**, *6*, 484–490.
30. Meldal, M.; Tornøe, C. W. Cu-Catalyzed Azide-Alkyne Cycloaddition. *Chem. Rev.* **2008**, *108*, 2952–3015.
31. Kamphuis, M. M. J.; Johnston, A. P. R.; Such, G. K.; Dam, H. H.; Evans, R. A.; Scott, A. M.; Nice, E. C.; Heath, J. K.; Caruso, F. Targeting of Cancer Cells Using Click-Functionalized Polymer Capsules. *J. Am. Chem. Soc.* **2010**, *132*, 15881–15883.
32. Wu, J.; Gao, C. Sliding Supramolecular Polymer Brushes with Tunable Amphiphilicity: One-Step Parallel Click Synthesis and Self-Assembly. *Macromolecules* **2010**, *43*, 7139–7146.
33. Wu, J.; He, H.; Gao, C. β-Cyclodextrin-Capped Polyrotaxanes: One-Pot Facile Synthesis via Click Chemistry and Use as Templates for Platinum Nanowires. *Macromolecules* **2010**, *43*, 2252–2260.
34. Davis, M. E.; Brewster, M. E. Cyclodextrin-Based Pharmaceutics: Past, Present and Future. *Nat. Rev. Drug Discovery* **2004**, *3*, 1023–1035.
35. Wattendorf, U.; Kreft, O.; Textor, M.; Sukhorukov, G. B.; Merkle, H. P. Stable Stealth Function for Hollow Polyelectrolyte Microcapsules through a Poly(ethylene glycol) Grafted Polyelectrolyte Adlayer. *Biomacromolecules* **2008**, *9*, 100–108.
36. Heuberger, R.; Sukhorukov, G.; Vörös, J.; Textor, M.; Möhwald, H. Biofunctional Polyelectrolyte Multilayers and Microcapsules: Control of Non-Specific and Bio-Specific Protein Adsorption. *Adv. Funct. Mater.* **2005**, *15*, 357–366.
37. Vyas, A.; Saraf, S.; Saraf, S. Cyclodextrin Based Novel Drug Delivery Systems. *J. Incl. Phenom. Macrocycl. Chem.* **2008**, *62*, 23–42.
38. Uekama, K.; Hirayama, F.; Irie, T. Cyclodextrin Drug Carrier Systems. *Chem. Rev.* **1998**, *98*, 2045–2076.
39. Harada, A.; Kamachi, M. Complex Formation between Poly(ethylene glycol) and α-Cyclodextrin. *Macromolecules* **1990**, *23*, 2821–2823.
40. Kalashnikov, P. A.; Sokolov, V. I.; Topchieva, I. N. Synthesis of Polyrotaxanes Based on α-Cyclodextrin and

Poly(ethylene oxide). *Russ. Chem. Bull. Int. Ed.* **2005**, *54*, 1973–1977.
41. Harada, A.; Li, J.; Kamachi, M.; Kitagawa, Y.; Katsube, Y. Structures of Polyrotaxane Models. *Carbohydr. Res.* **1998**, *305*, 127–129.
42. Staple, D.; Hanke, F.; Kreuzer, H. J. Complete Free Energy Landscape and Statistical Thermodynamics of Single Poly-(ethylene glycol) Molecules. *New J. Phys.* **2007**, *9*, 18–23.
43. Ortega-Munoz, M.; Lopez-Jaramillo, J.; Hernandez-Mateo, F.; Santoyo-Gonzalez, F. Synthesis of Glyco-Silicas by Cu(I)-Catalyzed "Click-Chemistry" and Their Applications in Affinity Chromatography. *Adv. Synth. Catal.* **2006**, *348*, 2410–2420.
44. Zelikin, A. N.; Li, Q.; Caruso, F. Disulfide-Stabilized Poly-(methacrylic acid) Capsules: Formation, Cross-Linking, and Degradation Behavior. *Chem. Mater.* **2008**, *20*, 2655–2661.
45. Ochs, C. J.; Such, G. K.; Caruso, F. Modular Assembly of Layer-by-Layer Capsules with Tailored Degradation Profiles. *Langmuir* **2011**, *27*, 1275–1280.
46. Hong, R.; Han, G.; Fernandez, J. M.; Kim, B.-J.; Forbes, N. S.; Rotello, V. M. Glutathione-Mediated Delivery and Release Using Monolayer Protected Nanoparticle Carriers. *J. Am. Chem. Soc.* **2006**, *128*, 1078–1079.
47. Yap, H. P.; Johnston, A. P. R.; Such, G. K.; Yan, Y.; Caruso, F. Click-Engineered, Bioresponsive, Drug-Loaded PEG Spheres. *Adv. Mater.* **2009**, *21*, 4348–4352.
48. Sivakumar, S.; Bansal, V.; Cortez, C.; Chong, S.-F.; Zelikin, A. N.; Caruso, F. Degradable, Surfactant-Free, Monodisperse Polymer-Encapsulated Emulsions as Anticancer Drug Carriers. *Adv. Mater.* **2009**, *21*, 1820–1824.
49. Caponovo, J.; Ruiz, J.; Cloutet, E.; Astruc, D. New Polyalkynyl Dendrons and Dendrimers: "Click" Chemistry with Azidomethylferrocene and Specific Anion and Cation Electrochemical Sensing Properties of the 1,2,3-Triazole-Containing Dendrimers. *Chem.—Eur. J.* **2009**, *15*, 2990–3002.
50. Harada, W.; Li, J.; Nakamitsu, T.; Kamachi, M. Preparation and Characterization of Polyrotaxanes Containing Many Threaded α-Cyclodextrins. *J. Org. Chem.* **1993**, *58*, 7524–7528.
51. Wang, Y.; Caruso, F. Nanoporous Protein Particles through Templating Mesoporous Silica Spheres. *Adv. Mater.* **2006**, *18*, 795–800.